Table 1.8 Parallel screening of a library of 120 self-assembled catalysts in the rhodium-catalyzed asymmetric hydrogenation by the classic approach.

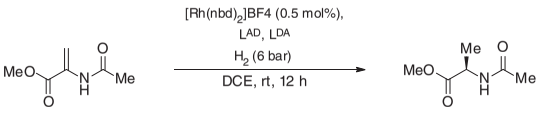

L^{DA}	L^{AD}	(*S*)-**17a**	(*S*)-**17b**	(*S*)-**17c**	(*S*)-**17d**	(*S*)-**17e**	(*S*)-**17f**	(*S*)-**16a**	(*S*)-**16b**	(*S*)-**16c**	(*S*)-**16d**	(*S*)-**16e**	(*S*)-**16f**
		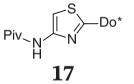 **17**						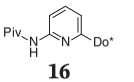 **16**					
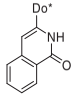 **18**	(*S*)-**18a**	**99 (quant.)**	96 (quant.)	95 (quant.)	88 (quant.)	**99 (quant.)**	79 (quant.)	**99 (86)**	97 (88)	96 (89)	89 (quant.)	**99 (90)**	81 (93)
	(*S*)-**18b**	90 (quant.)	91 (99)	90 (98)	92 (quant.)	90 (quant.)	84 (quant.)	92 (84)	89 (86)	91 (85)	86 (89)	93 (86)	85 (94)
	(*S*)-**18c**	94 (quant.)	82 (98)	88 (97)	90 (quant.)	95 (quant.)	88 (quant.)	94 (83)	93 (79)	87 (78)	88 (81)	90 (84)	81 (85)
	(*S*)-**18d**	92 (quant.)	88 (quant.)	81 (quant.)	66 (quant.)	91 (quant.)	60 (quant.)	89 (quant.)	84 (98)	85 (95)	54 (90)	88 (quant.)	40 (88)
	(*S*)-**18e**	**99 (quant.)**	94 (quant.)	92 (quant.)	89 (quant.)	98 (quant.)	90 (quant.)	**99 (89)**	98 (87)	94 (86)	84 (95)	**99 (92)**	79 (95)
	(*S*)-**18f**	87 (quant.)	89 (quant.)	90 (quant.)	80 (quant.)	88 (quant.)	78 (quant.)	93 (quant.)	95 (95)	94 (89)	81 (95)	89 (87)	74 (83)
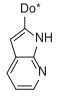 **19**	(*S*)-**19a**	90 (quant.)	87 (94)	90 (92)	41 (96)	91 (quant.)	76 (53)	88 (85)	87 (78)	91 (81)	46 (84)	87 (90)	79 (47)
	(*S*)-**19b**	82 (quant.)	77 (72)	85 (57)	49 (80)	81 (quant.)	39 (15)	84 (81)	83 (80)	89 (59)	55 (73)	85 (81)	48 (58)
	(*S*)-**19c**	78 (quant.)	66 (89)	74 (35)	37 (77)	79 (quant.)	36 (14)	80 (82)	71 (71)	77 (65)	49 (68)	82 (85)	20 (64)
	(*S*)-**19d**	81 (quant.)	81 (84)	84 (66)	52 (98)	82 (quant.)	43 (56)	83 (88)	82 (58)	86 (67)	38 (quant.)	80 (87)	44 (78)

Reaction conditions: $[Rh(nbd)_2]BF_4$, [Rh] : L^{AD} : L^{DA} : substrate = 1 : 1.05 : 1.05 : 200, H_2 (6 bar), DCE, c_0(substrate) = 0.3 M, 12 hours, RT. Enantioselectivity was determined by chiral GC, conversion was determined by ^{1}H NMR spectroscopy.

ee

(conv.)

Table 1.9 Combinational approach to the identification of the most active and selective ligand combinations in the rhodium-catalyzed asymmetric hydrogenation.

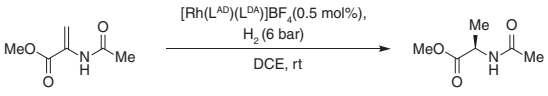

Step 1	L^{AD}	17	16
L^{DA}	Do	(*S*)-**17a** (*S*)-**17b** (*S*)-**17c** (*S*)-**17c** (*S*)-**17e** (*S*)-**17f**	(*S*)-**16a** (*S*)-**16b** (*S*)-**16c** (*S*)-**16c** (*S*)-**16e** (*S*)-**16f**
18	(*S*)-**18a** (*S*)-**18b** (*S*)-**18c** (*S*)-**18d** (*S*)-**18e** (*S*)-**18f**	84% *ee* (quant.)	79% *ee* (quant.)
19	(*S*)-**19a** (*S*)-**19b** (*S*)-**19c** (*S*)-**19d**	62% *ee* (92%)	

Step 2		17		
L^{DA}	Do	(*S*)-**17a** (*S*)-**17e**	(*S*)-**17b** (*S*)-**17d**	(*S*)-**17c** (*S*)-**17f**
18	(*S*)-**18a** (*S*)-**18e**	99% *ee*	93% *ee*	87% *ee*
	(*S*)-**18b** (*S*)-**18c**	92% *ee*	89% *ee*	89% *ee*
	(*S*)-**18d** (*S*)-**18f**	82% *ee*	84% *ee*	84% *ee*

Step 3		17	
L^{DA}	Do	(*S*)-**17a**	(*S*)-**17e**
18	(*S*)-**18a**	99% *ee*	99% *ee*
	(*S*)-**18e**	99% *ee*	98% *ee*

Reaction conditions: $[Rh(nbd)_2]BF_4$, [Rh] : L^{AD} : L^{DA} : substrate = 1 : 1.05 : 1.05 : 200, H_2 (6 bar), DCE, c_0(substrate) = 0.3 M, 12 hours, RT. Enantioselectivity was determined by chiral GC, conversion was determined by ^{1}H NMR spectroscopy.
The shades should highlight the conditions which gave the highest yield and enantioselectivity.

At room temperature, both diastereomeric complexes are indistinguishable, but at lower temperatures, one complex is favored.

The potential of this concept was shown in rhodium-catalyzed asymmetric hydrogenation. With the ligands **20S** and **20R,** enantiomeric excess up to 90% could be achieved (Table 1.10). Control experiments in MeOH showed how crucial hydrogen bonding is to achieve enantioselectivity.

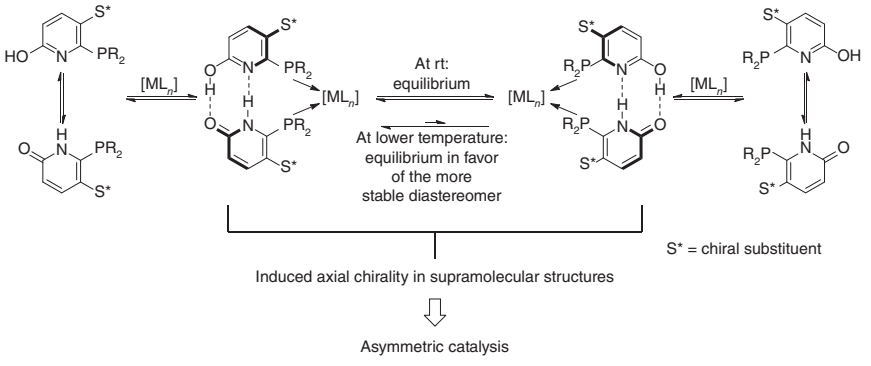

Scheme 1.10 Induced axial chirality in supramolecular structures.

Table 1.10 Asymmetric hydrogenation of methyl acetamidoacrylate.

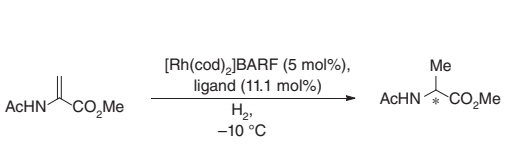

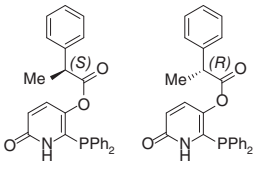

20S **20R**

#	Ligand	Solvent	Conversion (%)	*ee* (%)
1	**20S**	DCE	85	84 (*S*)
2	**20R**	DCE	81	85(*R*)
3	**20S**	*o*-DCB	93	90 (*S*)
4	**20S**	MeOH	1	*rac*.

[Rh]/L/substrate 1 : 2.2 : 20; *c*(substrate) = 0.02 M; conversion and ee determined by chiral-phase GC. BARF = *tetrakis*[3,5-*bis*(trifluoromethyl)phenyl]borate.

1.4 Other Catalytic Applications

Self-assembling ligands are not limited to rhodium-catalyzed hydroformylation or hydrogenation reactions. This methodology was successfully applied on several reactions.

1.4.1 Hydration of Alkynes

The addition of water to alkynes is an important way to install functional groups into a carbon skeleton. This transformation usually follows the Markovnikov rule [27–31]. An *anti*-Markovnikov selective hydration of a terminal alkyne would be a convenient method to generate aldehydes. For this unusual hydration mode, only few ruthenium catalysts were previously reported [32–37]. Bidentate ligands [35],

phosphinopyridine ligands [34], and the preorientation of the water molecule by hydrogen bonding [33] seemed to have positive effects in the reported processes. Self-assembling ligands also incorporate a pyridinyl-functionalized phosphine group, and they emulate bidentate ligands with their hydrogen bonding system, which might interact with water.

To obtain further insight, the hydration of 1-nonyne catalyzed by half-sandwich ruthenium complexes with different ligands was investigated [38]. With mono- or bidentate phosphine ligands, only low activity and selectivity were observed (Table 1.11, entries 1–3). The 6-DPPon ligand, which should be able to self-assemble by hydrogen bonding, showed similar results (entry 4). However, a catalyst based on the complementary self-assembling of the heterodimeric aminopyridine/isoquinolone ligands yielded the desired product in perfect selectivity with excellent catalyst activity (entry 5). By control experiments, it was shown that the heterodimeric ligand combination is responsible for the best catalyst (entries 6 and 7).

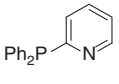

dppy

dppe

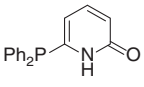

6-DPPon

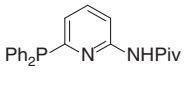

7a

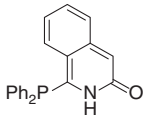

8a

Table 1.11 Ruthenium complex-catalyzed hydration of 1-nonyne.

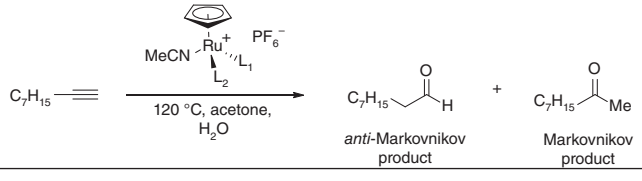

#	Cat.	L1	L2	*t* (h)	Aldehyde[a] (%)	Ketone[a] (%)
1		PPh_3	PPh_3	140	1.2	18
2[b]		dppy	dppy	168	4.0	2.4
3		dppe	—	168	2.1	20
4[b]		6-DPPon (**1**)	6-DPPon(**1**)	168	2.1	25
5		(**7a**)	(**8a**)	26	94	0
6[b]		(**7a**)	(**7a**)	72	39	3.8
7		(**8a**)	(**8a**)	48	1.9	0

a) Yield calculated from GC response factors relative to internal standard hexadecane.
b) κ^1-P, κ^2-P,N coordination of the phosphinopyridine with replacement of the acetonitrile ligand.

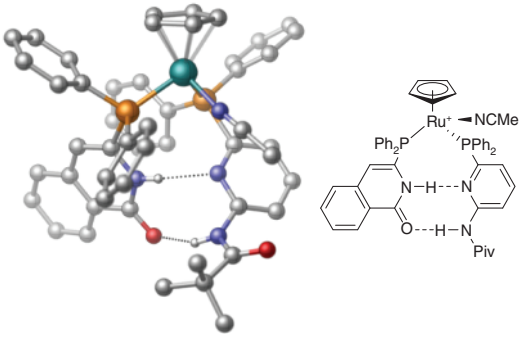

Figure 1.4 X-ray crystal structure of a [(Cp)Ru(**7a**)(**8a**)(NCMe)]$^{+}$-complex (carbon-bonded hydrogen atoms and the PF_6^- counterion are omitted for clarity.

The structure of the best catalyst was further analyzed by X-ray crystal structure analysis and the hydrogen bonding was confirmed (Figure 1.4). This catalyst was applied on a scope of 10 different alkynes with in almost all cases perfect chemoselectivity for the aldehyde and good-to-excellent activities.

1.4.2 Hydration of Nitriles

Classical hydration of nitriles to amides requires very harsh conditions [39]. Transition metal catalysis offers a powerful tool to perform this reaction under very mild conditions [40, 41]. For this reason, the hydration of nitriles to amides is an important example of an industrially important atom economic reaction [42]. After the successful application of the self-assembly ligands in the hydration of alkynes, it seemed promising to apply these ligands also to nitriles. For this reason, homo- and heterodimeric *bis*(acetylacetonato)ruthenium(II) complexes of the ligands **7a** and **8a** were prepared [43]. The structure of these complexes was investigated in solution and in solid state. Especially for the heterodimeric combination, some unusual hydrogen bonding patterns were observed involving hydrogen bonding in between the **8a** ligand and an oxygen atom of an acac ligand (Figure 1.5).

However, the homo-complex of **8a** showed the highest activity in the hydration of *p*-tolylcarbonitrile (Table 1.12).

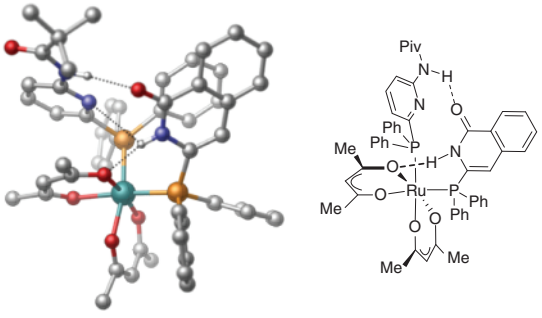

Figure 1.5 X-ray crystal structure of a [Ru(acac)$_2$(**7a**)(**8a**)]-complex (carbon-bonded hydrogen atoms are omitted for clarity) [43].

Table 1.12 Ruthenium complex-catalyzed hydration of nitriles.

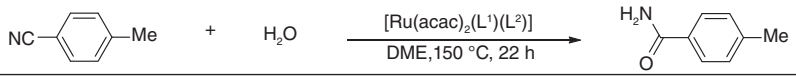

#	L^1	L^2	Conversion (%)	TOF (h^{-1})
1	**8a**	**8a**	100	20
2	**8a**	**7a**	90	5
3	**7a**	**7a**	<5	nd

Reaction conditions: $[Ru(acac)_2(L^1)(L^2)]$/substrate/water = 1 : 100 : 200, DME (1 ml), substrate (1 mmol), water (2 mmol), 150 °C, 22 hours.

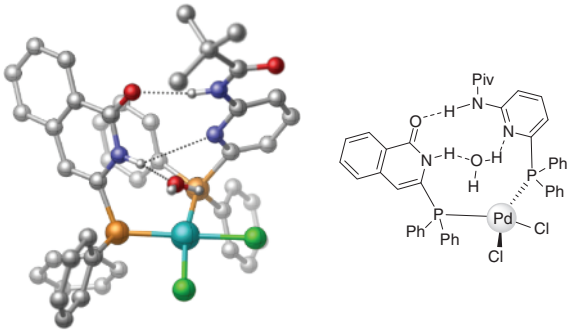

Figure 1.6 X-ray crystal structure of $[Cl_2Pd(\mathbf{8a}\cdot H_2O)(\mathbf{7a})]$ (carbon-bonded hydrogen atoms are omitted for clarity) [44].

1.4.3 Allylic Substitution with Allylic Alcohols

It was possible to synthesize crystals of a $[Cl_2Pd(\mathbf{8a}\cdot H_2O)(\mathbf{7a})]$ suitable for X-ray structure analysis (Figure 1.6) [44]. Interestingly, a single water molecule was incorporated in the hydrogen bonding system of the complementary self-assembly ligands.

Inspired by this interaction of water with the ligand backbone, it seemed reasonable that alcohols might form similar interactions [44]. Especially allylic alcohols might be directed by this interaction in a beneficial orientation with the palladium center. Indeed, it was possible to apply directly allylic alcohols as substrates in allylic substitution with water as the only by-product (Scheme 1.11). The common substrates of classic allylic substitution catalysts are in most cases allylic acetates or carbonates [45]. These substrates have to be prepared in an extra step and release always a stoichiometric amount of a coupled byproduct. The palladium-catalyzed allylic substitution with the self-assembly ligands can directly apply allylic alcohols and generates as stoichiometric by-product only water.

1.4.4 Hydrocyanation

The nitrile group is often found in many natural products as well as in different pharmaceuticals, agrochemical products, and functional materials [46]. The nitrile

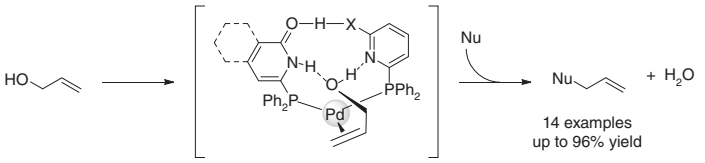

Scheme 1.11 Palladium complex-catalyzed allylic substitution of allylic alcohols directed by substrate pre-orientation through hydrogen bonding to self-assembled ligands.

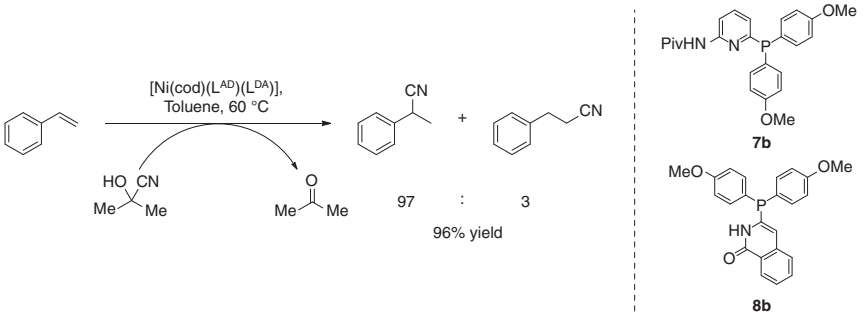

Scheme 1.12 Nickel complex-catalyzed hydrocyanation of alkenes.

group is also quite useful in organic synthesis because it can easily be transformed into different functional groups such as amines, aldehydes, ketones, and other carboxylic acid derivatives [47]. An elegant method to generate these molecules is the hydrocyanation of alkenes by the formal addition of HCN to a C=C double bond [48, 49]. Most industrial catalysts are based on (bidentate) phosphite or phosphinite ligands, but bidentate phosphine ligands showed also interesting reactivities [50]. Van Leeuwen et al. showed that electron poor bidentate ligands with bite angles around 105° seem to have positive results on the catalysts activity [51–53].

It has been demonstrated that the complementary heterodimeric self-assembly ligands can form Ni^0 complexes, which are promising catalysts in the hydrocyanation of styrenes [54]. A 5×4 ligand matrix of ligands derived from the isoquinolone and aminopyridine platform was used to identify the best ligand combination. The so found catalyst provided very high activity, perfect regioselectivity, and a good functional group tolerance in the nickel-catalyzed hydrocyanation of alkenes (Scheme 1.12). It is worth to highlight that the best ligand combination (**7b**/**8b**) bares electron-rich groups in contrast to previously reported catalysts, which seem to give better results with electron-poor ligands [52].

1.5 Concluding Remarks

In this chapter, the self-assembly of monodentate phosphine ligands in transition metal complexes by hydrogen bonding was described.

We have introduced the unique 6-DPPon ligand platform in homogeneous catalysis based on the homodimeric 2-pyridone/2-hydroxypyridine system. Catalysts

based on this platform showed an outstanding performance in rhodium-catalyzed hydroformylation of allenes, alkynes, and terminal alkenes, in some cases even at room temperature and under one atmosphere of syngas. Considering the limited accessibility of high-pressure equipment in many laboratories, this is a major advantage of this system. In addition, by introducing chiral substituents at the pyridone platform, an axial chiral self-assembled ligand system can be generated, which showed promising first results in asymmetric hydrogenation.

The A–T base pairing in the DNA inspired the complementary self-assembly of heterodimeric ligands. This approach offers easy access to the formation of structurally diverse ligand libraries. The huge advantage compared with classical bidentate ligands is that a catalyst composed of two unsymmetrical donors is easily realized just by mixing two complementary ligands together. For the synthesis of a comparable classic bidentate ligand with a covalent backbone and two unsymmetrical donor sites, a huge synthetic effort is necessary. Using these ligand libraries, it was possible to identify potent catalysts for many different transformations such as hydrocyanation, hydration of alkynes, or allylic substitution. Especially in rhodium-catalyzed hydroformylation, it was possible to generate outstanding active and selective catalysts. These catalysts enable perfect selectivity for the linear aldehyde even in protic solvents, which is an impressive proof for the stability of the supramolecular ligand backbone by hydrogen bonding. Nevertheless, large ligand libraries can still lead to a huge experimental effort to test all possible ligand combinations. In asymmetric hydrogenation, it was possible to give an example for the superiority of combinatorial methods to identify the most active catalyst, compared with the classical testing of all ligand combinations (17 instead of 120 reactions).

All those findings clearly show that the self-assembly of ligands by hydrogen bonding is a valuable tool for the synthetic chemist to use in homogeneous transition metal catalysis.

References

1 Hagen, J. (2015). Homogeneous catalysis with transition metal catalysts. In: *Industrial Catalysis: A Practical Approach*, 17–46. Weinheim, Germany: Wiley-VCH.

2 Hartwig, J.F. (2010). *Organotransition Metal Chemistry: From Bonding to Catalysis*. Mill Valley, California: University Science Books.

3 Schneider, H.-J. and Yatsimirsky, A.K. (2000). *Principles and Methods in Supramolecular Chemistry*. Chichester: Wiley.

4 Dydio, P. and Reek, J.N.H. (2014). Supramolecular control of selectivity in transition-metal catalysis through substrate preorganization. *Chem. Sci.* 5 (6): 2135–2145.

5 Lehn, J.-M. (1988). Supramolecular chemistry—scope and perspectives molecules, supermolecules, and molecular devices (nobel lecture). *Angew. Chem. Int. Ed. Engl.* 27 (1): 89–112.

6 Watson, J.D. and Crick, F.H. (1953). Molecular structure of nucleic acids; a structure for deoxyribose nucleic acid. *Nature* 171 (4356): 737–738.

7 Breit, B. and Seiche, W. (2003). Hydrogen bonding as a construction element for bidentate donor ligands in homogeneous catalysis: regioselective hydroformylation of terminal alkenes. *J. Am. Chem. Soc.* 125 (22): 6608–6609.

8 Gellrich, U., Seiche, W., Keller, M., and Breit, B. (2012). Mechanistic insights into a supramolecular self-assembling catalyst system: evidence for hydrogen bonding during rhodium-catalyzed hydroformylation. *Angew. Chem. Int. Ed. Engl.* 51 (44): 11033–11038.

9 Leeuwen, P.W.N.M. and Claver, C. (2002). *Rhodium Catalyzed Hydroformylation*. Dordrecht: Kluwer Academic Publishers.

10 Gellrich, U., Huang, J., Seiche, W. et al. (2011). Ligand self-assembling through complementary hydrogen-bonding in the coordination sphere of a transition metal center: the 6-diphenylphosphanylpyridin-2(1*H*)-one system. *J. Am. Chem. Soc.* 133 (4): 964–975.

11 Gellrich, U., Koslowski, T., and Breit, B. (2015). Full kinetic analysis of a rhodium-catalyzed hydroformylation: beyond the rate-limiting step picture. *Catal. Sci. Technol.* 5 (1): 129–133.

12 Gellrich, U., Himmel, D., Meuwly, M., and Breit, B. (2013). Realistic energy surfaces for real-world systems: an IMOMO CCSD(T):DFT scheme for rhodium-catalyzed hydroformylation with the 6-DPPon ligand. *Chemistry* 19 (48): 16272–16281.

13 Beierlein, C.H., Breit, B., Paz Schmidt, R.A., and Plattner, D.A. (2010). Online monitoring of hydroformylation intermediates by ESI-MS. *Organometallics* 29 (11): 2521–2532.

14 Seiche, W., Schuschkowski, A., and Breit, B. (2005). Bidentate Ligands by self-assembly through hydrogen bonding: a general room temperature/ambient pressure regioselective hydroformylation of terminal alkenes. *Adv. Syn. Catal.* 347 (11–13): 1488–1494.

15 Straub, A.T., Otto, M., Usui, I., and Breit, B. (2013). Room temperature ambient pressure (RTAP)-hydroformylation in water using a self-assembling ligand. *Adv. Syn. Catal.* 355 (10): 2071–2075.

16 Agabekov, V., Seiche, W., and Breit, B. (2013). Rhodium-catalyzed hydroformylation of alkynes employing a self-assembling ligand system. *Chem. Sci.* 4 (6): 2418.

17 Köpfer, A. and Breit, B. (2015). Rhodium-catalyzed hydroformylation of 1,1-disubstituted allenes employing the self-assembling 6-DPPon system. *Angew. Chem. Int. Ed. Engl.* 54 (23): 6913–6917.

18 Breit, B. and Seiche, W. (2005). Self-assembly of bidentate ligands for combinatorial homogeneous catalysis based on an A-T base-pair model. *Angew. Chem. Int. Ed. Engl.* 44 (11): 1640–1643.

19 Waloch, C., Wieland, J., Keller, M., and Breit, B. (2007). Self-assembly of bidentate ligands for combinatorial homogeneous catalysis: methanol-stable platforms analogous to the adenine–thymine base pair. *Angew. Chem.* 119 (17): 3097–3099.

20 Weis, M., Waloch, C., Seiche, W., and Breit, B. (2006). Self-assembly of bidentate ligands for combinatorial homogeneous catalysis: asymmetric rhodium-catalyzed hydrogenation. *J. Am. Chem. Soc.* 128 (13): 4188–4189.

21 Wieland, J. and Breit, B. (2010). A combinatorial approach to the identification of self-assembled ligands for rhodium-catalysed asymmetric hydrogenation. *Nat. Chem.* 2 (10): 832–837.

22 Tang, W. and Zhang, X. (2003). New chiral phosphorus ligands for enantioselective hydrogenation. *Chem. Rev.* 103 (8): 3029–3070.

23 Berthod, M., Mignani, G., Woodward, G., and Lemaire, M. (2005). Modified BINAP: the how and the why. *Chem. Rev.* 105 (5): 1801–1836.

24 Miyashita, A., Yasuda, A., Takaya, H. et al. (1980). Synthesis of 2,2′-bis (diphenylphosphino)-1,1′-binaphthyl (BINAP), an atropisomeric chiral bis(triaryl)phosphine, and its use in the rhodium(I)-catalyzed asymmetric hydrogenation of .alpha.-(acylamino)acrylic acids. *J. Am. Chem. Soc.* 102 (27): 7932–7934.

25 Miyashita, A., Takaya, H., Souchi, T., and Noyori, R. (1984). 2, 2'-bis (diphenylphosphino)-1, 1'-binaphthyl(binap). *Tetrahedron* 40 (8): 1245–1253.

26 Wenz, K.M., Leonhardt-Lutterbeck, G., and Breit, B. (2018). Inducing axial chirality in a supramolecular catalyst. *Angew. Chem. Int. Ed. Engl.* 57 (18): 5100–5104.

27 Blum, J., Huminer, H., and Alper, H. (1992). Alkyne hydration promoted by RhCl3 and quaternary ammonium salts. *J. Mol. Catal.* 75 (2): 153–160.

28 Casado, R., Contel, M., Laguna, M. et al. (2003). Organometallic gold(III) compounds as catalysts for the addition of water and methanol to terminal alkynes. *J. Am. Chem. Soc.* 125 (39): 11925–11935.

29 Mizushima, E., Sato, K., Hayashi, T., and Tanaka, M. (2002). Highly efficient AuI-catalyzed hydration of Alkynes. *Angew. Chem. Int. Ed.* 41 (23): 4563–4565.

30 Hartman, J.W., Hiscox, W.C., and Jennings, P.W. (1993). Catalytic hydration of alkynes with platinum(II) complexes. *J. Org. Chem.* 58 (26): 7613–7614.

31 Fukuda, Y. and Utimoto, K. (1991). Effective transformation of unactivated alkynes into ketones or acetals with a gold(III) catalyst. *J. Org. Chem.* 56 (11): 3729–3731.

32 Alvarez, P., Bassetti, M., Gimeno, J., and Mancini, G. (2001). Hydration of terminal alkynes to aldehydes in aqueous micellar solutions by ruthenium(II) catalysis; first anti-Markovnikov addition of water to propargylic alcohols. *Tetrahedron Lett.* 42 (48): 8467–8470.

33 Grotjahn, D.B., Incarvito, C.D., and Rheingold, A.L. (2001). Combined effects of metal and ligand capable of accepting a proton or hydrogen bond catalyze anti-Markovnikov hydration of terminal alkynes. *Angew. Chem. Int. Ed.* 40 (20): 3884–3887.

34 Grotjahn, D.B. and Lev, D.A. (2004). A general bifunctional catalyst for the anti-Markovnikov hydration of terminal alkynes to aldehydes gives enzyme-like rate and selectivity enhancements. *J. Am. Chem. Soc.* 126 (39): 12232–12233.

35 Suzuki, T., Tokunaga, M., and Wakatsuki, Y. (2001). Ruthenium complex-catalyzed anti-Markovnikov hydration of terminal alkynes. *Org. Lett.* 3 (5): 735–737.

36 Tokunaga, M., Suzuki, T., Koga, N. et al. (2001). Ruthenium-catalyzed hydration of 1-alkynes to give aldehydes: insight into anti-Markovnikov regiochemistry. *J. Am. Chem. Soc.* 123 (48): 11917–11924.

37 Tokunaga, M. and Wakatsuki, Y. (1998). The first anti-Markovnikov hydration of terminal alkynes: formation of aldehydes catalyzed by a ruthenium(II)/phosphane mixture. *Angew. Chem. Int. Ed.* 37 (20): 2867–2869.

38 Chevallier, F. and Breit, B. (2006). Self-assembled bidentate ligands for Ru-catalyzed anti-Markovnikov hydration of terminal alkynes. *Angew. Chem. Int. Ed. Engl.* 45 (10): 1599–1602.

39 Green, M.M. and Wittcoff, H.A. (2006). *Organic Chemistry Principles and Industrial Practice*, 1e. Weinheim: Wiley-VCH.

40 Ahmed, T.J., Knapp, S.M.M., and Tyler, D.R. (2011). Frontiers in catalytic nitrile hydration: Nitrile and cyanohydrin hydration catalyzed by homogeneous organometallic complexes. *Coord. Chem. Rev.* 255 (7-8): 949–974.

41 Kukushkin, V.Y. and Pombeiro, A.J.L. (2002). Additions to metal-activated organonitriles. *Chem. Rev.* 102 (5): 1771–1802.

42 Trost, B.M. (2002). On inventing reactions for atom economy. *Acc. Chem. Res.* 35 (9): 695–705.

43 Šmejkal, T. and Breit, B. (2007). Self-assembled bidentate ligands for ruthenium-catalyzed hydration of nitriles. *Organometallics* 26 (9): 2461–2464.

44 Usui, I., Schmidt, S., Keller, M., and Breit, B. (2008). Allylation of N-heterocycles with allylic alcohols employing self-assembling palladium phosphane catalysts. *Org. Lett.* 10 (6): 1207–1210.

45 Trost, B.M. and Crawley, M.L. (2003). Asymmetric transition-metal-catalyzed allylic alkylations: applications in total synthesis. *Chem. Rev.* 103 (8): 2921–2944.

46 Fleming, F.F. (1999). Nitrile-containing natural products. *Nat. Prod. Rep.* 16 (5): 597–606.

47 Larock, R.C. (1999). *Comprehensive Organic Transformations: A Guide to Functional Group Preparations*, 2e. New York, NY: Wiley-VCH.

48 Torborg, C. and Beller, M. (2009). Recent applications of palladium-catalyzed coupling reactions in the pharmaceutical, agrochemical, and fine chemical industries. *Adv. Syn. Catal.* 351 (18): 3027–3043.

49 Zhang, H., Su, X., and Dong, K. (2020). Recent progress in transition-metal-catalyzed hydrocyanation of nonpolar alkenes and alkynes. *Org. Biomol. Chem.* 18 (3): 391–399.

50 Goertz, W., Kamer, P.C.J., van Leeuwen, P.W.N.M., and Vogt, D. (1997). Application of chelating diphosphine ligands in the nickel-catalysed hydrocyanation of alk-l-enes and ω-unsaturated fatty acid esters. *Chem. Commun.* (16): 1521–1522.

51 Freixa, Z. and van Leeuwen, P.W.N.M. (2003). Bite angle effects in diphosphine metal catalysts: steric or electronic? *Dalton Trans.* (10): 1890–1901.

52 Goertz, W., Keim, W., Vogt, D. et al. (1998). Electronic effects in the nickel-catalysed hydrocyanation of styrene applying chelating phosphorus ligands with large bite angles. *J. Chem. Soc., Dalton Trans.* (18): 2981–2988.

53 Kranenburg, M., Kamer, P.C.J., van Leeuwen, P.W.N.M. et al. (1995). Effect of the bite angle of diphosphine ligands on activity and selectivity in the nickel-catalysed hydrocyanation of styrene. *J. Chem. Soc., Chem. Commun.* (21): 2177.

54 de Greef, M. and Breit, B. (2009). Self-assembled bidentate ligands for the nickel-catalyzed hydrocyanation of alkenes. *Angew. Chem. Int. Ed. Engl.* 48 (3): 551–554.